

## N O T I C E

THIS DOCUMENT HAS BEEN REPRODUCED FROM  
MICROFICHE. ALTHOUGH IT IS RECOGNIZED THAT  
CERTAIN PORTIONS ARE ILLEGIBLE, IT IS BEING RELEASED  
IN THE INTEREST OF MAKING AVAILABLE AS MUCH  
INFORMATION AS POSSIBLE

# NASA

Technical Memorandum 80624

## The Penrose Photoproduction Scenario for NGC 4151: A Black Hole Gamma Ray Emission Mechanism for Active Galactic Nuclei and Seyfert Galaxies

**D. Leiter**

(NASA-TM-80624) THE PENROSE PHOTOPRODUCTION  
SCENARIO FOR NGC 4151: A BLACK HOLE  
GAMMA-RAY EMISSION MECHANISM FOR ACTIVE  
GALACTIC NUCLEI AND SEYFERT GALAXIES (NASA)  
33 p HC A02/MF A01

N80-17938

Unclas  
12886

CSCI 03B G3/90

**DECEMBER 1979**

National Aeronautics and  
Space Administration

**Goddard Space Flight Center**  
Greenbelt, Maryland 20771



THE PENROSE PHOTOPRODUCTION SCENARIO FOR NGC 4151:  
A BLACK HOLE  $\gamma$ -RAY EMISSION MECHANISM FOR ACTIVE  
GALACTIC NUCLEI AND SEYFERT GALAXIES

Dr. Darryl Leiter(\*)  
Laboratory for High Energy Astrophysics  
NASA/Goddard Space Flight Center  
Greenbelt, Maryland 20771  
USA

(8) NAS/NRC Resident Research Associate

## SUMMARY

On the basis of general arguments, it has been suggested (Bignami, Fichtel, Hartman, and Thompson 1979) that a steepening of the spectrum between X-ray and Gamma ray energies may be a general,  $\gamma$ -ray characteristic of Seyfert galaxies, if the diffuse Gamma ray spectrum is considered to be a superposition of unresolved contributions, from one or more classes of extragalactic objects.

In the following work, we will show that the above suggestion can be given a consistent theoretical interpretation in the context of the Penrose Photoproduction Scenario PPS, (Leiter, Kafatos 1979). Specifically in the case of NGC 4151, the dominant process will be shown to be Penrose Compton Scattering PCS in the ergosphere of a  $M \geq 10^8 M_{\odot}$  Kerr black hole, assumed to exist in the Seyfert's active galactic nucleus. (KEY WORDS -- BLACK HOLES, ACTIVE GALAXIES, GAMMA RAY BURSTS, SEYFERTS )

### I. Introduction

It has recently been conjectured (Bignami, Fichtel, Hartman, and Thompson, 1979), that if we assume the isotropic diffuse Gamma radiation contains significant, unresolved contributions from one or more classes of active extragalactic objects, then this assumption requires a "steepening" of the spectral index of the active galactic sources in the superposition, over the  $\sim 2$  MeV to  $\sim 3$  MeV region. Individual data on active galaxies suggest this as well.

In this paper we will show how this conjectured constraint, on active galactic sources, can be made plausible in the context of the "Penrose Photoproduction Scenario" PPS. Specifically we will show that for the case of Seyfert galaxies, like NGC 4151, PPS is most likely dominated by the low energy component,

namely Penrose Compton Scattering PCS. PCS will occur if massive, central, rapidly spinning Kerr Black Holes ( $M \geq 10^8 M_\odot$ ), (surrounded by hot ( $T \sim 10^9$  K) accretion disks, with turbulent, optically thin inner regions), exist in the Seyfert active galactic nuclei. Under these conditions, Seyfert (PCS)  $\gamma$ -ray emissions are generated stochastically, for ( $300 \text{ keV} < E < 3 \text{ MeV}$ ), with burst times of  $\Delta t_{\text{PCS}} \geq (2.2 \text{ hrs}) M_8$ , (where  $M = M_8 \times 10^8 M_\odot$ ). The characteristic PCS cutoff ( $< 3 \text{ MeV}$ ), is strongly controlled by the electron mass. This "universal" PCS cutoff gives astrophysical support to the above mentioned "steepening" conjecture. Since galactic PCS scenarios allow ( $M_8 \geq 1$ ), the associated stochastic  $\gamma$ -ray transient can range over time intervals greater than several hours.

## II. The "Penrose Photoproduction Scenario" PPS

In a series of recent publications, (Leiter and Kafatos, 1978, Kafatos and Leiter 1979, Leiter and Kafatos 1979), the Penrose Photoproduction Scenario PPS, for active galactic nuclei, was developed on the basis of two plausible assumptions:

- a) a massive, rotating Kerr black hole ( $10^8 M_\odot < M < 10^{10} M_\odot$ ) is generated by normal accretion processes, in the central region of a young galaxy, and has an equilibrium (angular momentum density/per unit mass) value of  $a/M \lesssim 0.998$ ; (Thorne 1974).
- b) an accretion disk surrounds this "canonical" Kerr black hole and, during the active period, generates a very hot, optically thin, spatially thick inner region. This inner region of the accretion disk is unstable and turbulent, and sporadically injects hot plasma and blueshifted radiation into the inner regions of the ergosphere of the Kerr black hole.

Under these two assumptions it is possible to have "Penrose

Compton Scattering" (PCS), (Piran, Shaham 1977) and "Penrose Pair Production" (PPP) (Leiter, Kafatos 1978; Kafatos, Leiter 1979). These two processes comprise the "Penrose Photoproduction Scenario" (PPS), (Leiter, Kafatos 1979); which boosts the conventional accretion-radiation mechanisms, so that a substantial fraction of the total luminosity occurs in the X-ray and gamma ray regions.

The ergosphere around a Kerr black hole has the fundamental property that local inertial frames are dragged around with respect to the rotational sense of the black hole, relative to a local inertial frame at infinity. In fact, it is this relativistic "frame dragging" effect, between the inside and the outside of the ergosphere, which causes the effective energy boost to occur in Penrose Photoproduction. An LNRF observer<sup>(\*)</sup> tied to an inertial frame inside the ergosphere, will see copious, high energy photoproduction processes occurring, since photons which enter the ergosphere are strongly blueshifted. For example, in the case of a Kerr black hole with  $a/M = (1 - \frac{\delta^3}{4})$ ;  $\delta \ll 1$ , a photon of energy  $E_{ph}$  and angular momentum  $L_{ph}$  arriving at the radius  $r = M(1+\delta)$ , near the equator inside the ergosphere, will be blueshifted by the formula

$$E = [(E_{ph} - \omega L_{ph}) / [\delta / 2a - \delta^3]]^{1/2} \quad (1)$$

where  $\omega = 1/2M$  and  $\delta \ll 1$ . Since the target region lies just outside the event horizon, in the co-ordinate zone bounded by the marginally bound and marginally stable orbits, then  $(\delta^{3/2} < \epsilon < \delta)$ . For a "canonical" Kerr black hole with  $a/M = 0.998$  then  $\delta = 0.2$ , and the effective photon blueshifting in the target zone can range from 10 to 30 times the energy of the incoming photons. These blueshifted photons can act to trigger photoproduction processes on electron

(\*) An observer in a "local non-rotating frame" such that the local metric is of a diagonal form, allowing local proper time and length to be known.

and proton targets falling into the target region due to accretion. This is because the "proper thickness" of the target zone is large, (Leiter, Kafatos 1979), (Leiter, Kafatos 1978), (Piran, Shaham 1977)

$$D \approx M \left[ \ln \left( \frac{1}{\sqrt{f}} \right) \right] \approx (0.8 M) \quad (2)$$

A lower bound on the  $\gamma$ -ray emission time, for Penrose Compton Scattering PCS, can be obtained by dividing equation (2) by the speed of light, since this is the lower bound on the time it takes plasma blobs to cross the Penrose Photoproduction target region, in a quasi-Keplerian orbit, this is seen to be,

$$\Delta t_{pps} \geq (2.2 M_8) \text{ hrs.} \quad (3)$$

PCS generates  $\gamma$ -ray transients, (300 keV to  $\sim 3$  MeV), with times of  $\Delta t_{PCS} \geq (2.2 \text{ hrs}) M_8$ , into a solid angle bounded above and below the equator of the Kerr black hole by  $\sim 40^\circ$ , as will be discussed below, (see figure 1).

Hence if the observer lies within this "Penrose focusing angle" he sees the PCS Gamma ray "bursts". On the other hand, if the observer does not lie within this Penrose focusing angle, he will see only the X-ray output of the accretion disk, as defining the upper limit of his observed continuum spectrum, since the PCS Gamma rays will not enter his detector.

Of fundamental importance is the fact that Penrose Photoproduction processes have natural emission cutoffs, occurring in the energy of the ejected particle, which is strongly controlled by the mass of the particle, recoil-injected into a negative energy orbit thru the event horizon. For the case of PCS around large black holes ( $M_8 > 1$ ), this cutoff is on the order of  $\sim 3$  MeV, and for kinematic reasons will be strongly dependent on the electron mass, (i.e. this is the particle which is recoil-injected into the event horizon by the PCS process).

### III. The Seyfert Galaxy NGC 4151 and the Penrose Photoproduction Scenario (PPS)

#### The Penrose Photoproduction Scenario

PPS contains two processes, a low energy one, Penrose Compton Scattering PCS, a high energy one, Penrose Pair Production PPP

The high energy process PPP is associated with the generation of high energy ( $\lesssim$  GeV) bursts of  $e^{\pm}$ , and their associated conversion into bursts of Gamma rays (on the order of GeV), and strong, highly variable compact radio source emission. Since such high energy Gamma rays, on the order of GeV, are not seen from NGC 4151 and since its radio emission is weak, almost constant (Beall, 1979), it would appear that the high energy PPP component of PPS is not present in NGC 4151. However the low energy component PCS could be present since X-rays as high as 60 keV have been observed from NGC 4151 (Mushotzky, Holt, Serlemitsos, 1978). This suggests that NGC 4151 could have a hot ( $T \approx 10^9$  K) inner region in its accretion disk, since disk models exist which can generate X-rays in a  $< 100$  keV range (Eardley, Lightman, Payne, Shapiro, 1978). For these accretion disk models with ( $T \approx 10^9$  K), the most likely component of PPS is the Penrose Compton Scattering PCS process, while its companion high energy process PPP would be very unlikely to occur in this disk scenario. This occurs because these temperature ranges allow the inner region of the accretion disk to generate hard X-rays  $\sim 100$  keV, then after blue-shifting is taken into account, the plasma injected into the target region will see photons with energies in the range of  $\sim 1$  MeV. In this energy range, if the optical depth for photon-photon absorp-



tion is not too large, the most likely photo-production processes seen in the LNR frame is Compton scattering. This occurs because the criteria for this to be a Penrose PCS process is that the recoiling particles (electrons for PCS) be injected into negative energy, retrograde, Penrose orbits, while the escaping particles (photons for PCS) are ejected with energy boosts picked up from the rotational energy of the Kerr black hole. Kinematically this requires that the recoil particle be given a velocity boost, as seen in the LNRF, of at least half the speed of light. This requires the blueshifted photon to have an energy ( $\sim \frac{1}{2}$  MeV) the order of the rest energy of the recoil injected electron.

From the above arguments we see that the observed X-ray and radio properties of NGC 4151 suggest that the disk temperature is such that only the low energy PCS component can be present.

The Photon flux/keV, "F(E)", as seen above the atmosphere, emanating from an active galaxy, is usually defined

$$F(E) = \left[ \dot{N}(E) / 4\pi R_g^2 \right] \text{ (photons/cm}^2\text{-sec-keV)} \quad (4)$$

where  $\dot{N}(E)$  is the galactic spectral photon spectrum (photons/sec-keV) at energy E, and  $R_g$  is the galactic distance from the detector, (in cm). In the case of photon "bursts", over  $\Delta t$ (sec),  $N(E)$  can also be related to the corresponding galactic photon emission spectrum  $N(E)$

$$\dot{N}(E)_{(Burst)} = \frac{N(E)_{(Burst)}}{\Delta t_{(Burst)}} \quad (5)$$

Hence equations (4) and (5) can be combined to give a relationship between F(E) and N(E) during a PCS burst

$$F(E)_{(PCS)} = \left[ N(E)_{(PCS)} \cdot (\Delta t_{(PCS)} 4\pi R_g^2) \right] \quad (6)$$

From equation (4), (5) and (6) we note the following fact: if

$F(E)_{(PCS)}$  is observed to obey an  $E^{-p}$  burst spectrum, then this implies  $N(E)_{(PCS)} \sim E^{-p}$ ,  $N(E)_{(PCS)} \sim E^{-p}$  as well. Hence it will be sufficient to discuss the spectra of  $N(E)_{(PCS)}$  for comparison to observations on  $F(E)_{(PCS)}$

Secondly, for the purposes of our discussion, we briefly review the results of the detailed Monte Carlo calculations on PCS (Piran, Shaham 1977 a,b). They showed that in the case of "small" ( $M \sim 10M_{\odot}$ ) Kerr black holes, surrounded by hot accretion disks which generate hard X-rays, that (in a "canonical" scenario with "radial" photons hitting "circular" electrons) a PCS boosted  $\gamma$ -ray burst would be generated, whose spectral index was harder than that of the input X-rays from the disk.

The "canonical" PCS spectral power law index was shown to range from about  $E^{-3}$  to  $E^{-2}$  when generated on input X-rays, from an optically thin bremsstrahlung disk (Payne and Eardley 1977), with  $N_x(E) \sim (e^{-E/KT})/E$  and  $KT = 50$  keV. The hardest  $E^{-2}$  spectrum corresponds to optical depths in the ergosphere of  $\tau_{*} \approx 3$ , so that the average number of PCS scatterings per photon was  $\sim 2$ , (see Figures 2,3,4,5). Their Monte Carlo calculations showed that the PCS spectral index could be hardened above that of the "canonical" case by taking into account the contribution of incoming photons with retrograde (instead of just radial) motion, or by increasing the energy of the incoming photon distribution above that of  $T = 50$  keV.

It was also shown that the spectrum could be further hardened again by any mechanism which could give the target electron some positive radial momentum. This could occur thru induced temperature effects via "plasma relaxation" in the plasma blob, since  $(h/mc^2) \ll \Delta t(\text{plasma instabil. time}) < \Delta t(\text{electron, proton cooling time})$  is valid, in the  $10^9$ K plasma as it falls through the Penrose target region ( $r_{mb} < r < r_{ms}$ ). When plasma relaxation induces temperature effects in PCS, the initially scattered PCS electron can be

re-scattered, by the plasma protons and magnetic fields, from retrograde negative energy orbits back into positive energy prograde orbits. In this way they participate in more PCS with positive values of radial momentum, and hence harden the PCS spectrum above that of the purely "canonical" PCS case where the target electrons move in purely circular orbits. In all cases, the majority of the PCS photons are emitted in a zone 40 degrees above and below the black hole equator when  $(a/M)$  obeys  $(0.95 < a/M \leq 0.998)$ . When "Plasma Hardening" occurs, the maximum PCS  $\gamma$ -ray energy will be larger than that of the canonical case due to the fact that the associated multiple PCS scattering can combine both the "angular momentum escape condition" and the "radial escape PCS conditions", thus leading to a maximum PCS energy above that of the optimal canonical case  $\approx 4.3 m_e c^2 \approx 2.2$  MeV. The most efficient case was shown to be for  $\tau_* = 3$ , (with an average of two PCS per photon), giving an upper cutoff energy of  $\approx 5.2 m_e c^2 \approx 2.7$  MeV. In general, since the PCS burst spectrum has an input directly from the hard X-ray spectrum of the inner accretion disk, then the intensity of the PCS burst is automatically normalized to this hard X-ray intensity, times a PCS "Photon Efficiency" factor which was shown to vary from (0.05 to 0.47), depending on the optical depths chosen in the ergosphere. The maximum photon efficiency was realized for the case of optical depths in the ergosphere of  $\tau_* = 3$ , while for  $\tau_* = 1$ , photon efficiencies of about 0.1 were realized.

We now apply these facts to the case of an active galaxy (like NGC 4151) by scaling up the previous results to the  $M_B > 1$  range. The justification for this procedure is due to the fact that

properties of the PCS Monte Carlo model for small black holes will scale with the Kerr black hole  $M$  and  $a/M$  values. This is also true of the various accretion disk scenarios, which depend on the ratio of  $M$ , ( $\dot{M}/M$ ) and  $a/M$  (Eardley, Lightman, Payne, Shapiro (1978). However, in the case of  $M_{\text{BH}} \gtrsim 10^6 M_{\odot}$  expected for galactic black holes, the efficiency of the "plasma hardening" effect improves with regard to its spectral hardening capability. This is because when the Kerr black hole is in its PCS efficient range ( $0.95 < a/M \leq 0.998$ ), then the efficiency of the plasma hardening effect is tied to the amount of time that the plasma blob spends in passing thru the PCS target region. Since this time factor is related to the size of the Penrose target region  $D \approx (0.8)M$ , the plasma blob will spend more time undergoing PCS, and its associated plasma hardening, in  $M_{\text{BH}} \gtrsim 10^6 M_{\odot}$  Kerr black holes, than in the  $M_{\text{BH}} \approx 10^7 M_{\odot}$  Kerr black holes considered by Piran and Shaham. For this reason, in the  $M_{\text{BH}} \gtrsim 10^6 M_{\odot}$  case, the input hard X-ray spectrum will be more efficiently boosted by  $\Lambda(\text{PCS})$ , above that of the "canonical" case, in regard to its spectral index. Our algorithm generated, from scaling up the PCS Monte Carlo calculations, shows that the hard X-ray spectrum in the (50 keV to 200 keV) region is boosted into the  $\sim$ MeV region, up to a  $\leq 3$  MeV cutoff. In the case of NGC 4151, since the hard X-ray spectral input index is  $E^{-1.4}$  (Mushotzky 1978), this implies that, when  $\tau^* \gtrsim 1$ , the PCS gamma ray burst spectral index will be harder than the input X-ray spectrum of 1.4, up to a universal cutoff at  $\leq 3$  MeV. The universal  $\leq 3$  MeV cutoff can be understood as due to multiple "plasma hardened" re-scattering of electrons in the target region, during PCS, occurring around a massive canonical Kerr black hole with  $M \gtrsim 10^8 M_{\odot}$ , in conjunction with optimum optical depths and

the smooth, almost constant, (PCS) kinematic escape behavior, associated with the range ( $0.95 < a/M \leq 0.998$ ) for Kerr black holes  $M_B \geq 1$ . For NGC 4151, if  $M_B \geq 1$ , then the PCS burst spectrum will be harder than the X-ray input of  $E^{-1.4}$ , all the way up to the 3 MeV cutoff, since the phase space for PCS escape will be "saturated" by plasma hardening in this regime.

Analysis of recent balloon observations of NGC 4151 suggests that if  $\sim$  MeV  $\gamma$ -rays are present, they are probably variable and have "high state" spectrum of  $F(E) \sim E^{-1}$ , with a cutoff in the  $\leq 3$  MeV, see figure 6. It is, at this time, still difficult to judge the accuracy of these observations due to the short time base of observations on NGC 4151. This is because the PCS  $\gamma$ -ray bursts could well be varying stochastically over time periods of hours, (recall that  $\Delta t_{\text{PCS}} \geq (2.2 \text{ hrs}) M_B$ , while ( $M_B \geq 1$ )). Hence, present balloon observations can serve only as a preliminary means to test the PCS model in NGC 4151. While the possibility exists that extended balloon flights might improve the situation (J. Kurfess private comm), it will take future satellite experiments (e.g. NASA/GRO) to accurately study PCS in NGC 4151, and other active galaxies as well. Nonetheless, on the basis of present balloon data, the existence and variability of the  $\sim E^{-1}$  "hard tail," in the MeV region, for NGC 4151 up to the  $\leq 3$  MeV cutoff in the spectrum, might be given a plausible, astrophysical interpretation in terms of the optimal, "plasma hardened" saturated PCS burst model, for a  $M_B \geq 1$  Kerr black hole in its active nucleus.

We can determine the required accretion rate  $\dot{M}$  needed to run the PCS process. This can be estimated by noting that for the hot optically thin disks we envisage, (Payne, Eardley, 1974),

we have in the  $T \sim 10^9$  K regime that the luminosity in X-rays of energy  $E_{ph}$ , can be related to the accretion rate  $\dot{M}_1$  ( $M_\odot/\text{yr}$ ) as  $L = (L_{44} \times 10^{44} \text{ erg/sec})$ ,

$$L_{44} (E_{ph} \approx (60 \text{ keV}) R^{1/2}) \approx \dot{M}_1 \approx 1.7 (M_\odot \text{ yr}^{-1}) \quad (7)$$

where  $R$  is the Eddington ratio  $R = L/L_{\text{Edd}} = (0.6 \dot{M}_1/M_\odot)$ . Since we observe X-rays, in the (50 keV to 100 keV) region, emitted from NGC 4151,  $\approx 10^{43}$  ergs/sec, then this allows the reasonable values of  $\dot{M}_1 \approx 0.1$  and  $(0.1 < R < 0.4)$  to apply to our PCS scenario described above. The average value of the PCS photon flux 'keV is related to the accretion disk X-ray flux by

$$F_{\text{PCS}} (1 \text{ MeV}) = \eta_{\text{PCS}} F_x (100 \text{ keV}) \quad (8)$$

where  $\eta_{\text{PCS}}$  is the photon number efficiency for (PCS). Using the data of (Perotti et al., 1979) as a measure of the strength of the PCS bursts we find that

$$\eta_{\text{PCS}} \approx (0.1) \quad (9)$$

which is in a range compatible with the Monte Carlo values ( $1 < \tau_* < 3$ ) ( $0.05 < \eta_{\text{PCS}} < 0.5$ ), (Piran, Shaham 1977). Hence we see that the PCS mechanism contains a reasonable set of operating parameters, for the observed X-rays, and  $\gamma$ -ray bursts, seen from NGC 4151.

To test the consistency of the plasma hardened saturated PCS mechanism for NGC 4151 against another important physical process, namely photon-photon absorption by pair production, we note that the optical depths for the latter process, can be estimated by the method of (Heterich 1974) to be

$$\tau_{\gamma\gamma'} \approx \frac{\left[ 5 R_g^2 F_{\gamma'} (E_{\gamma'} (\text{keV})) \right]^{E_{\gamma'} \approx (10^6/E_{\gamma'} (\text{keV}))}}{M_\odot c_\infty E_{\gamma'} (\text{keV})} \times 10^{-44} \quad (10)$$

where  $R_g$  is the distance of the active galaxy from the observer;  
 $M = M_g \times 10^8 M_\odot$  is the mass of the associated central Kerr black hole;  
 $E_\gamma$  (keV) and  $E_{\gamma'}$  (MeV) are the energies of the photons which collide  
 at  $r = (r^*)r_g$ ,  $r_g = (1.5 \times 10^{13} \text{ cm}) M_g$ ; and  $F_{\gamma'} [E_{\gamma'} (\text{keV})] E_{\gamma'} (\text{keV}) = \left( \frac{10^6}{E_{\gamma'} (\text{keV})} \right)$   
 is the associated observed flux of  $\gamma'$  photons which  
 emanate from the active galaxy. The value of  $\tau_{\gamma\gamma'}$  for the maximum  
 energy  $E_\gamma = (E_{\text{PCS}})_{\text{max}}$  ( $E_\gamma \approx 3000 \text{ keV}$   $\gamma$ -ray photons) to undergo  
 photon-photon absorption, is related to the flux of ( $E_{\gamma'} \approx 333 \text{ keV}$ )  
 hard x-rays contained in the accretion disk and its immediate vicin-  
 ity. Since  $R_g = 15 \text{ MPC} = 4.6 \times 10^{25} \text{ cm}$  and, (from Figure 6)  $F_{\gamma'} (\text{obs}) (333 \text{ keV})$   
 $\leq 10^{-5}$  (photons/cm<sup>2</sup>-sec-keV) for NGC 4151 then

$$\tau_{\gamma\gamma'} (\overrightarrow{3 \text{ MeV}}, \overleftarrow{333 \text{ keV}}) \leq \frac{6}{M_g R_g} \quad (11)$$

For the reasonable values of ( $r^* \sim 10$ ), associated with photon-  
 photon absorption outside the ergosphere (Eardley, et al 1978)

$$\tau_{\gamma\gamma'} (\overrightarrow{3 \text{ MeV}}, \overleftarrow{333 \text{ keV}}) \leq \frac{0.6}{M_g} \quad (12)$$

In the PCS model, we wish the PCS  $\gamma$ -rays to escape the disk,  
 without being "cutoff" by photon-photon absorption, so that its  
 efficiency in producing  $\gamma$ -rays is unabated. This means that we  
 require  $\tau_{\gamma\gamma'} (3 \text{ MeV}; 333 \text{ keV}) < 1$ , which requires ( $M_g \geq 0.6$ ). This  
 constraint is reasonable, since the allowed range of  $M_g$  values  
 in PPS in general is ( $1 < M_g < 100$ ), (i.e.  $10^8 M_\odot < M < 10^{10} M_\odot$ ).  
Hence if  $M \geq 6 \times 10^7 M_\odot$  is the mass of the central Kerr black hole in  
NGC 4151, then  $\tau_{\gamma\gamma'} < 1$  and the  $\leq 3 \text{ MeV}$   $\gamma$ -ray "cutoff" observed  
in the (PCS) burst will be unaffected by photon-photon  
absorption.

Note that while (PCS) does have a time dependent overall  
 "burst" output of  $\Delta t_{\text{PCS}} \geq (2.2 \text{ hrs}) M_g$ , its specific ( $\leq 3 \text{ MeV}$ )

"cutoff" is essentially constant in time and should be the same for each burst. This distinguishes the PCS  $\gamma$ -ray burst mechanism from other viable mechanisms for NGC 4151, such as the Compton-scattering model suggested by (Pinkau 1979), where the spectrum and its cutoff could vary widely in time, for different bursts, and allows future observations of NGC 4151 to test this unique PCS prediction.

From the data points, plotted in Figure 6, we see that there is the possibility of an implied variability associated with the MeV observations of NGC 4151, (e.g. Perotti et al., (1979), Della Ventura, et al (1979) see  $E \leq 3$  MeV Gamma rays during a time of 3 hrs, while (Zanrosso, et al., 1979) do not see  $E \leq 3$  MeV  $\gamma$ -rays for two 6 hour observations separated by 24 hrs.

Together these two observations suggest that possibly the PCS bursts are ranging over  $\geq 3$  hrs, separated by stochastic periods  $\geq 24$  hrs. The latter possibility is also made plausible by the fact that time variations (Mushotzky et al., 1978) in the 2-60 keV x-rays from the accretion disk, can vary on the order of days, (since this is also a possible measure of the plasma injection time into the PCS target region. This data is consistent with PCS, ( $M_g \geq 1$ ) with NGC 4151 emitting variable,  $\leq 3$  MeV  $\gamma$ -ray transients over durations on the order  $\Delta t_{PCS} \geq (2.2 \text{ hrs}) M_g$  separated by delay periods, (or "off" times), stochastically generated by the accretion disk, on the order of days. This interpretation might explain the apparent variability in the recent balloon data and suggests that future satellite borne experiments are needed to ultimately prove the hypothesis of  $M_g \geq 1$ , Kerr black hole induced PCS  $\gamma$ -ray bursts in NGC 4151.



Finally, we can estimate the strength of the induced radio source associated with PCS in NGC 4151 by noting that if the radio output is associated with  $e^\pm$  pairs made by photon-photon absorption from collisions between PCS gamma rays and hard X-rays from the disk, then the most efficient scenario requires them to be made just above the accretion disk, where they can escape into the outer region and be picked up by the available electric and magnetic fields (associated with "electromagnetic pump" mechanisms, like that of (Lovelace, 1976, 1979) ).

Using equation (12) and  $M_g \geq 3$ , we have that the number of pairs/sec made by photon-photon absorption is

$$\dot{N}_{e^\pm} = 4\pi R_g^2 (1 - e^{-\tau_{\gamma\gamma}}) E F_{PCS}(E) \Big|_{E \approx 3000 \text{ keV}} \quad (13)$$

And since  $R_g \approx 5 \times 10^{25} \text{ cm}$ ;  $F_{PCS}(3000 \text{ MeV}) \approx 3 \times 10^{-6} \frac{\text{photons}}{\text{cm}^2 \text{-sec-MeV}}$  ;  
for NGC 4151, then PCS generates

$$\dot{N}_{e^\pm} \lesssim (10^{50}) e^\pm/\text{sec} \quad (14)$$

in NGC 4151, from photon-photon absorption induced from PCS .

The radio output can be estimated as

$$L_{\text{radio}} \approx 2E_{\text{radio/chg}} \dot{N}_{e^\pm} \text{ (erg/sec)} \quad (15)$$

where  $E_{\text{radio/chg}}$  is the effective radio energy radiated/per charge. Since for NGC 4151,  $L_{\text{radio}} \sim 10^{38} \text{ erg/sec}$  (Beall, 1979), this requires  $E_{\text{radio/chg}} \lesssim 1 \text{ (eV/e}^\pm)$  which is very reasonable. Hence PCS could supply the necessary charges to generate a weak radio source powered by electron-positron pairs, which would give the observed zero Faraday rotation required (Noerdlinger, 1978).

The associated electron-positron cloud, generated by this process, will tend to be much longer lived than that of an equivalent number of pairs injected into a plasma, and hence will tend to generate 0.5 MeV line radiation after the pairs leak out of the radio region, into the ambient medium of the outer galaxy. If we assume the pairs in (14) eventually annihilate to produce 0.5 MeV lines, then after taking into account another factor of 0.25 for the singlet versus the triplet state, this yields

$$F_{\text{line}}(0.5 \text{ MeV}) \lesssim 10^{-3} \left( \frac{\text{photons}}{\text{cm}^2\text{-sec}} \right) \quad (16)$$

This might be seen by HEAO-C, and will be certainly observable by more sensitive instruments.

Hence if NGC 4151 has an electron-positron powered radio source, in this (PCS) induced fashion, it is possible that (0.5) MeV lines might be seen emanating from it, as well as MeV  $\gamma$ -rays.

#### IV. The Possible Relationship of Seyfert (PCS) to the Diffuse Gamma Ray Background

We now see that if PCS is the basic source of gamma ray bursts from Seyfert galaxies like NGC 4151, the universal  $\sim 3$  MeV cutoff, associated with this process, is consistent with the conjecture of Bignami, Fichtel, Hartman and Thompson (1979) that Seyferts might be able to account for most of the diffuse background up to the  $\sim$  MeV region. A preliminary application of the Photoproduction Scenario to quasars (like 3C273), was developed

elsewhere, (Leiter, Kafatos 1979, Kafatos, 1980). This work and (Swanenburg, 1978) suggests that both PCS and PPP may be active in quasars, and hence may be able to contribute significantly to the diffuse background above  $\sim 3$  MeV. Since detailed calculations for 3C273 are in process, we'll concentrate only on the Seyfert contribution in this paper. Suppose that we define the average active  $\sim 100$  keV X-ray lifetime of the hot accretion disk, around the Kerr black hole, inside the Seyfert galaxy as  $T_x$ . Then during a certain portion of this time,  $T_{(PCS)}$ , the PCS  $\gamma$ -ray burst process will be operating, if  $a/M$  is high enough (i.e.  $0.95 < a/M \leq 0.998$ ). This will cause PCS gamma ray bursts to be emitted ( $\sim 300$  keV to  $\sim 3$  MeV) in a solid angle made up of the area 40 degrees above and below the Kerr black hole equator (see figure 1, again). If there are a large number of Seyfert galaxies operating on PCS in this manner, so as to produce a diffuse background of X-rays and gamma-rays up to a  $\sim 3$  MeV cutoff, then because of the anisotropic emission associated with PCS, the number of  $\overset{N_{\gamma x}}{\wedge}$  gamma-ray burst emitting Seyferts which are observed will form a ratio to the number of  $\overset{N_x}{\wedge}$  x-ray continuum emitting Seyferts observed as

$$N_{\gamma} / N_x \sim \frac{\Omega_{PCS}}{4\pi} \left( \frac{T_{(PCS)}}{T_x} \right) \quad (17)$$

where  $\Omega_{PCS} \sim 4\pi(\cos 50^\circ) = 0.64$  is the effective solid angle into which the (PCS) gamma rays are emitted for each Seyfert. Hence we see that  $\frac{N_{\gamma x}}{N_x} = (0.64) \left( \frac{T_{(PCS)}}{T_x} \right)$  of the Seyfert X-ray galaxy population will contribute to the diffuse gamma-ray background  $300 \text{ keV} < E < 3 \text{ MeV}$ . With the coming of the NASA/GRO, it will be possible to make a catalogue of X-ray and gamma-ray

emitting Seyferts. One could then treat  $(\frac{N_{\gamma X}}{N_X})$  as an observed quantity and solve (17) for the average (PCS) lifetime ratio for Seyferts as

$$\left(\frac{T_{\text{PCS}}}{T_X}\right)_{\text{obs}} = (1.6)(N_{\gamma X}/N_X)_{\text{obs}} \quad (18)$$

This ratio  $(\frac{T_{\text{PCS}}}{T_X})_{\text{obs}}$  could be thought of as due to lifetime effects associated with the gradual slowing down of the Kerr black holes below the marginal value of  $a/M = 0.95$  needed to run the PCS process, or due to the gradual fall off, due to star formation, of the accretion rates  $\dot{M}$  needed to run the hot inner regions of the accretion disks, or both. Hence future observational knowledge from NASA/GRO will be helpful in formulating self-consistent dynamical calculations, in which the time dependence of the accretion disks and the Kerr black hole  $a/M$  ratios are taken into account in the PCS context.

#### V. Conclusions

We have shown how, for Seyferts like NGC 4151, Penrose Compton Scattering PCS can boost the hard X-ray spectrum in an  $M \gtrsim 10^8 M_\odot$  central Kerr black scenario into the MeV region in the form of  $\gamma$ -ray transients which range over a time interval  $\Delta t_{\text{PCS}} \gtrsim (2M_8)$  hours, up to a universal cutoff  $\leq 3$  MeV. These PCS  $\gamma$ -ray outbursts should come stochastically, corresponding to turbulent injection into the (PCS) target region of plasma blobs from the inner disk; hence the stochastic "off" times in between PCS "bursts" should be related to characteristic fluctuation times (e.g. X-ray fluctuation times) in the disk. In general, the spectral index of the gamma-ray PCS "burst" will be harder than that of the associated

hot disk X-ray spectral index, when optical depths in the ergosphere are of order unity. In all cases the PCS bursts are focused into a solid angle which extends 40 degrees above and below the Kerr black hole equator. This mechanism is consistent with recent balloon observations of NGC 4151 if  $M \gtrsim 10^8 M_\odot$ , with  $\dot{M} = 0.1 (M_\odot/\text{yr})$  and a PCS photon efficiency of about 10%. However, it will take more extensive long term balloon observations, and/or satellite experiments (e.g. NASA/GRO), which can see both the "off" and the "on" PCS states in the same experiment, to accurately corroborate the existence of this mechanism. But should this be possible, it may constitute the first solid observational test for the existence of a massive Kerr black hole, as a power source for Seyfert galaxies, since its characteristic signature is a  $\lesssim 3$  MeV cutoff which is the same for each PCS burst. This differs from other mechanisms which might attempt to explain the cutoff (e.g. Inverse Compton, Photon-Photon absorption, etc.) in the constancy of the cutoff, and in the ability of the PCS mechanism to explain the source of the power from which the output comes (e.g. the angular momentum energy of a Kerr black hole via its ergosphere).

If NGC 4151 is representative of Seyferts in general, this supports the conjecture of Bignami, Fichtel, Hartman and Thompson (1979) that Seyfert galaxies may be able to account for a very large part (if not all) of the diffuse gamma ray background, up to  $\lesssim 3$  MeV. Future calculations on quasars, like 3C273, with respect to the presence of the full Penrose Photoproduction Scenario, PPP and PCS, are in progress, and will show whether

the predicted  $\sim$  MeV and  $\sim$  GeV  $\gamma$ -rays are consistent with recent observations (Swanenburg, 1978). If it should turn out to be the case, then it may be that quasars may contribute significantly to the diffuse gamma ray spectrum above 3 MeV, up into the GeV region. It is also possible (Brown, & Stecker, 1979) that the diffuse background contains a cosmological component which cannot be ignored; however, one would first have to correct the observed diffuse background for known and projected point source contributions before being able to accurately apply and interpret the extent of such cosmological contributions. To this end, the NASA/GRO will make its greatest contribution, since in cataloguing the nature and number of point source contributions in the gamma-ray background it will at the same time most clearly define the cosmological component of the background which remains. This will lead to a clearer understanding of the dual role which the Penrose Photoproduction Scenario may play, in conjunction with cosmological mechanisms, in generating the diffuse gamma-ray background.

### Acknowledgements

The author wishes to thank Reuven Ramaty of the Laboratory for High Energy Astrophysics, NASA/Goddard Space Flight Center, for many stimulating conversations and useful suggestions during the developmental phase of this work. He also expresses thanks to Carl Fichtel of NASA/GSFC and James Kurfess of NRL for several interesting discussions on the interpretation of observational data associated with NGC 4141 and active galaxies.

## Figure Captions

- Fig. 1. An optically thin accretion disk with a hot, turbulent inner region, surrounds a massive Kerr black hole;  $M_g > 1$ ,  $a/m \leq 0.998$ . Hot plasma blobs and blue shifted photons are injected sporadically into the Penrose target region ( $r_{mb} < r < r_{ms}$ ) and cause PCS to occur. The resultant  $\gamma$ -ray bursts are focused into an angle of  $\sim 40^\circ$  above and below the equator, and range over  $\sim 300$  keV to  $\sim 2.7$  MeV. Mild photon-photon absorption, between PCS  $\gamma$ -rays and hard X-rays emitted perpendicularly from the disk yield a low density  $e^\pm$  cloud which can act as long-lived, weak, compact radio source with zero Faraday rotation. Photon-photon absorption, however, is in general insufficient (if  $M_g > 1$  for NGC 4151) to prevent large numbers of PCS  $\gamma$ -rays from escaping to infinity, where they are seen as  $\sim$  MeV  $\gamma$ -ray bursts acting stochastically over  $\geq (2.2 M_g)$  hrs.
- Fig. 2. "Canonical" PCS as seen in the (LNRF) in the "Penrose Target Region"  $r_{mb} \leq r \leq r_{ms}$ .  $\gamma$  is the incoming blue-shifted photon impinging on the orbiting ( $v_\phi \leq c/2$ ) electron  $e$ ,  $\gamma'$  is the PCS photon about to turn, leaving ergosphere, since it gave the scattered electron  $e'$  the required  $\Delta v \approx c/2$  boost to a negative energy retrograde orbit. The differential rotational sense  $\omega$  of the Kerr black hole,  $a/m \leq 0.998$ , is seen along the axis of rotation.
- Fig. 3. "Canonical" PCS as seen in the local electron rest frame (ERF), moving with  $v_\phi \leq c/2$  with respect to (LNRF). Compton scattering cross sections are first evaluated in the (ERF)



and then Lorentz transformed to the(LNRF) to determine the PCS processes that occur, then finally transformed to an observer, at infinity, in the Boyer-Lindquist frame.

Fig. 4. Monte Carlo calculations for "canonical" PCS for small  $M_g \sim 10^{-7}$  Kerr black holes,  $a/M = 0.998$ . The solid curve represents the accretion disk output ( $T_{ph} = 50$  keV), assumed to be blackbody in this case, and the dashed curve represents the PCS boosted "burst" output (taken from Piran, Shaham, 1977a). The boosted spectrum is always of a harder spectral index than that of the disk output for optical depths in the ergosphere of  $\tau_* \gtrsim 1$ . These results scale up directly with the  $M_g$  and  $\dot{M}_1$  values in the model, as long as  $a/M = 0.998$  is valid, and therefore can all be applied directly to massive galactic case where  $M_g \gtrsim 1$ . All spectra are associated with an observer at infinity, in an asymptotically flat spacetime.

Fig. 5 Similar calculations, as that of Figure 4, except with an optically thin bremsstrahlung accretion disk (Payne, Eardley, 1977) which can emit harder X-rays, up to a few hundred keV, in its own right. The resulting PCS burst spectrum is accordingly harder than the disk X-ray spectrum when  $\tau_* \gtrsim 1$ . Again these results will scale up into the massive  $M_g \gtrsim 1$  galactic black hole region ( $a/M = 0.998$ ) for the same reasons as given in Figure 4.

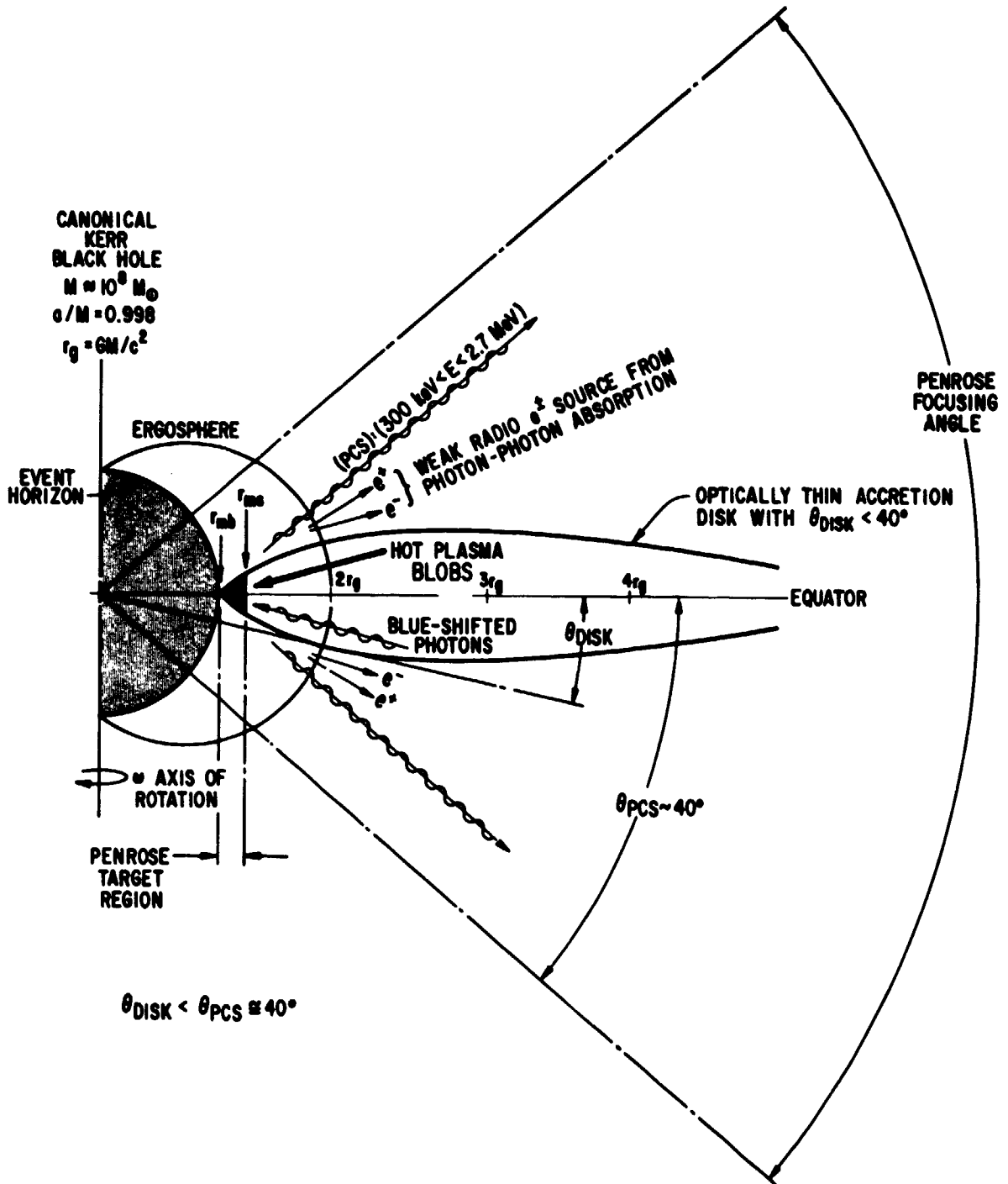
Fig. 6. Summary of recent data on NGC 4151

The solid curve represents the spectral shape of the 'PCS "burst" generated (via the  $M_g \approx 1$  PCS Monte Carlo algorithm) using the  $E^{-1.4}$  X-ray spectrum as input. The "dip" at  $\sim 300$  MeV is associated with the falloff of the hot accretion ( $E^{-1.4}$ ) disk spectrum (dotted line for  $\gtrsim 200$  keV) and the "pickup" in the PCS spectrum at  $\gtrsim 300$  keV. However, this "dip" could be disguised, in more general cases by mild Comptonization processes, and may not be universal. The PCS "cutoff"  $\lesssim 3$  MeV, however, is expected to be universal and hence should reveal itself in each  $\gamma$ -ray "burst" for an  $M_g \gtrsim 1$ , "phase space saturated," optimal PCS spectrum. This universal cutoff  $\lesssim 3$  MeV is a distinctive feature of PCS processes around massive  $M_g \gtrsim 1$  Kerr black holes and, if corroborated by future intercontinental balloon or satellite experiments, could be used as evidence for the existence of a massive  $M_g \gtrsim 1$  Kerr black hole in the nucleus of NGC 4151.

### References

- Auriemma, G., et al. 1978, Ap. J. Lett 221, L7.  
 Beall, J.H. (1979), NASA TM-80569 (GSFC).
- Bignami, G.F., Fichtel, C.E., Hartman, R.A. and Thompson, D.J.  
 (1979), Ap. J. 232, 649.
- Blandford, R.D. and Znajek, R.L. (1977), M.N.R.A.S. 179, 433.
- Della Ventura, Perotti, Villa, Baker, Butler, Dean, Martin,  
 Ramsden, Di Cocco (1979), 16th. Int. Cosmic Ray Conf.,  
 Kyoto I, 113.
- Eardley, D.M., Lightman, A.P., Payne, D.G. and Shapiro, S.L.  
 (1978) Ap. J. 224, 53.
- Gursky, H., Kellogg, E., Murray, S., Leong, E., Tannanbaum, H.  
 and Giacconi, R. (1971), Ap. J. Lett. 167, L81.
- Heterich, K. (1974), Nature 250, 311
- Kafatos, M. and Leiter, D. (1979), Ap. J. 229, 46. ((PPP), a/m = 0.998 case).  
 Kafatos, M., (1980), Ap. J. in press for Feb. 15, 1980 issue.  
 Ives, J.C., Sanford, P.W. and Preston, M.V. (1976), Ap. J. Lett.  
207, L159.
- Leiter, D. and Kafatos, M. (1978), Ap. J. 226, 32. ((PPP), a/m = 1 case)
- Leiter, D. and Kafatos, M. (1979), see article on full (PPS) scenario, in  
 Proc. La Jolla Institute, "Workshop on Particle Acceleration  
 Mechanisms in Astrophysics," (1979), #56, pg. 417.
- Lovelace, R.V.E. (1976), Nature 262, 649. Also see Proc. La Jolla Inst.  
 1979, A.I.P. Conf. # 56, page 399.
- Mushotsky, R.F., Holt, S.S. and Serlemitsos, P.J. (1978),  
 Ap. J. Lett. 225, L115.
- Noerdlinger, P. (1978), Phys. Rev. Lett. 41, 134.
- Payne, D.G. and Eardley, D.M. (1977), Ap. J. Lett. 19, 39.  
 Paciesas, W. S., Mushotzky, R. F., Pelling, R. M. (1977) M.N.R.A.S. 178, 23.  
 Piran, T. and Shaham, J. (1977a), Phys. Rev. 16-D, 1615.

- Piran, T. and Shaham, J. (1977b), Ap. J. 214, 268.
- Pinkau, K. (1979), Int. Cosmic Ray Conf., Kyoto, I, 165.
- Perotti, A. Della Ventura, G. and Sechi, G. (1979), NATURE,  
VOL. 282, 484. ----- see also Della Ventura  
et al (1979), quoted above.
- Crown, R.W., Stecker, F.W., (1979), Phys. Rev. Lett. 43, 315.
- Swanenburg, B.N. (1978), Nature 275, 314.
- Thorne, K. (1974), Ap. J. 191, 507.
- Zanroso, E.M., Long, J.L., Zych, A.D., Gibbons, R., White, R.S.  
and Dayton, B. (1979), Int. Cosmic Ray Conf, Kyoto, I,  
112.



THE NGC 4151 PENROSE COMPTON SCATTERING SCENARIO

Fig. 1

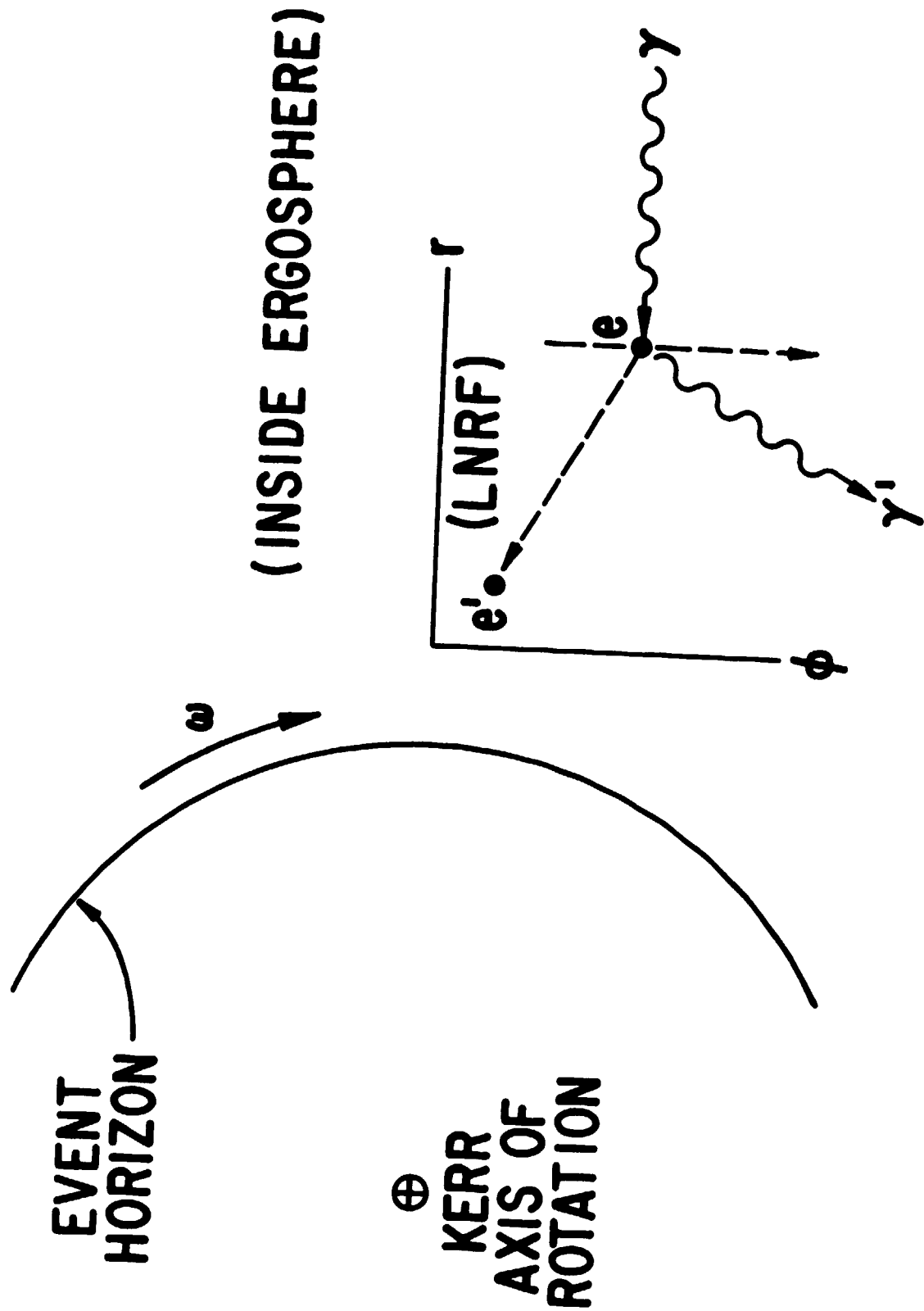


Fig. 2

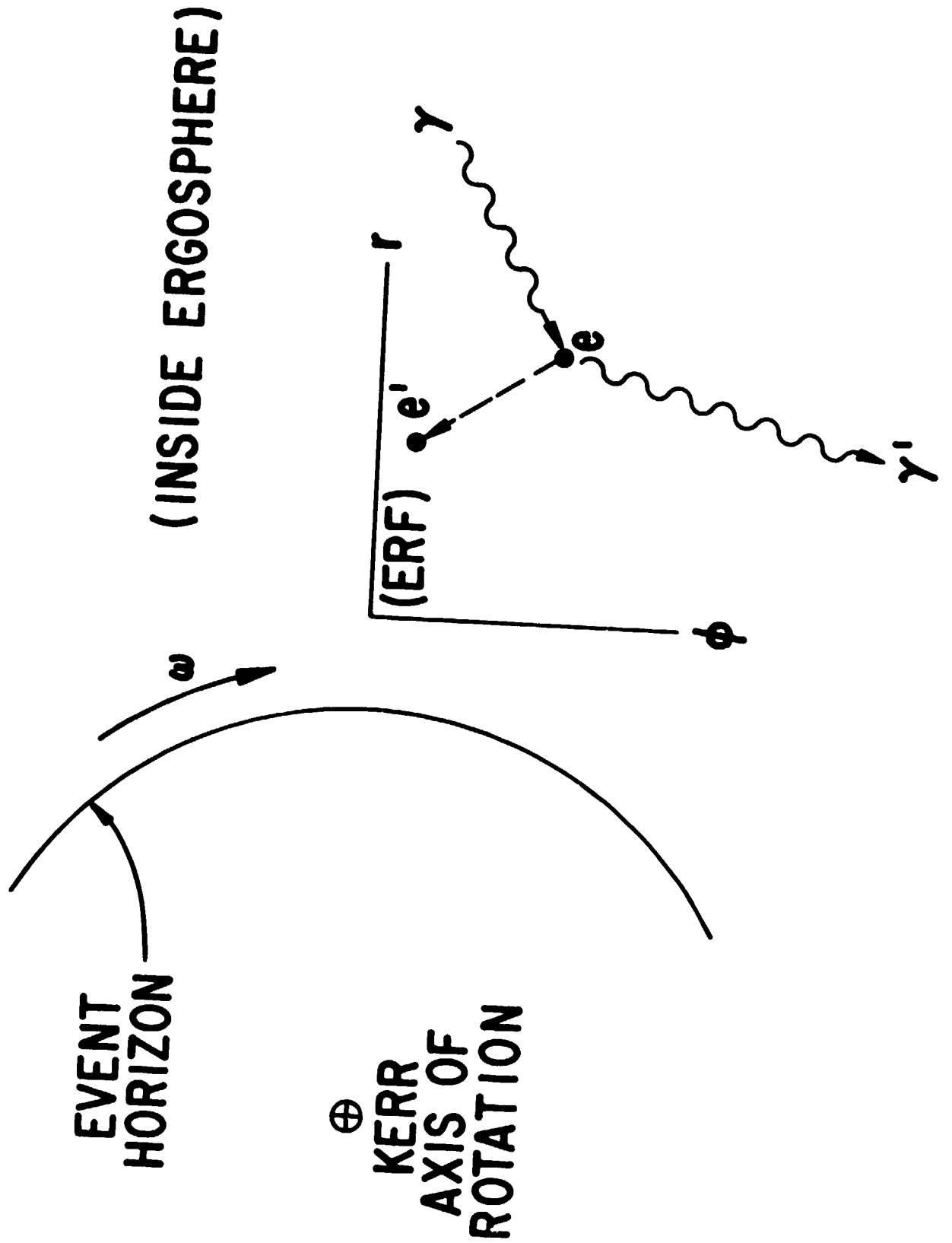


Fig 3

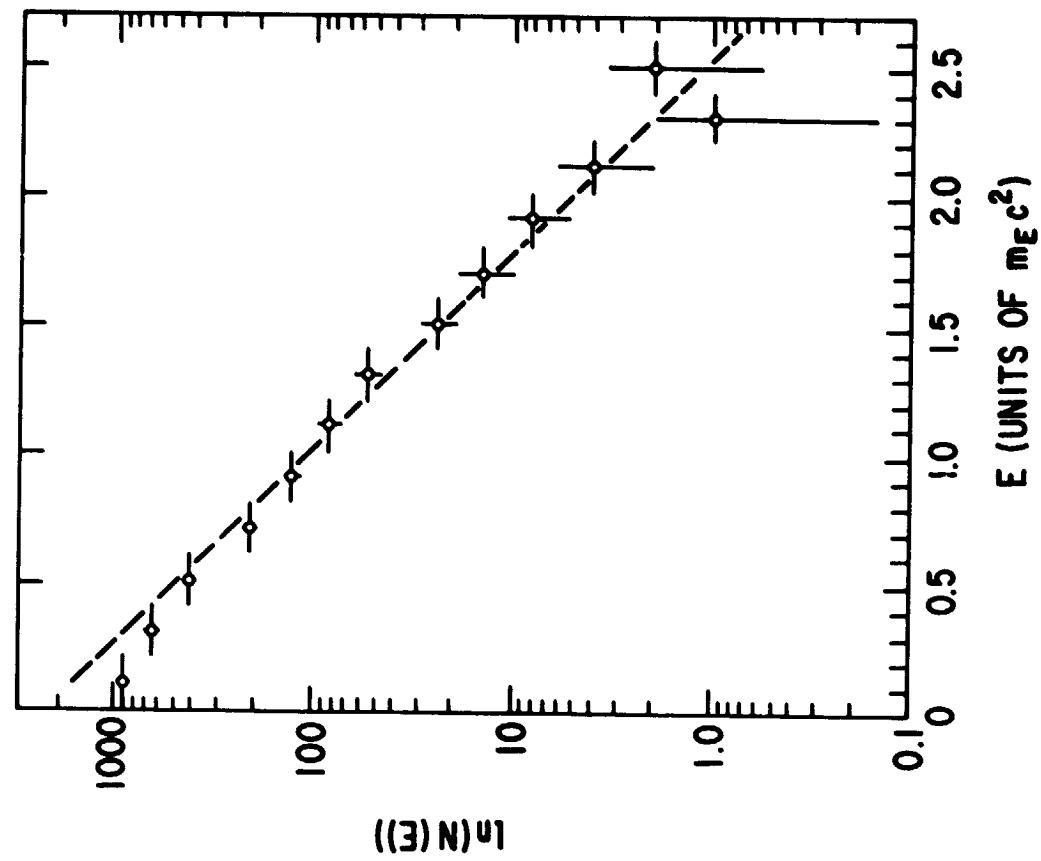


Fig. 5

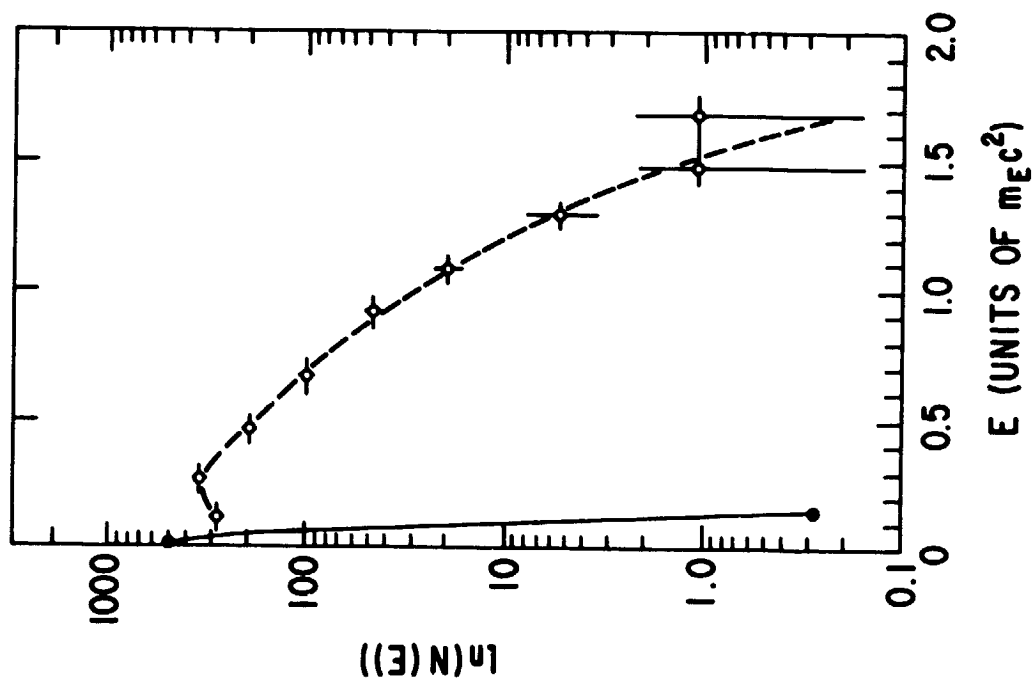


Fig. 4



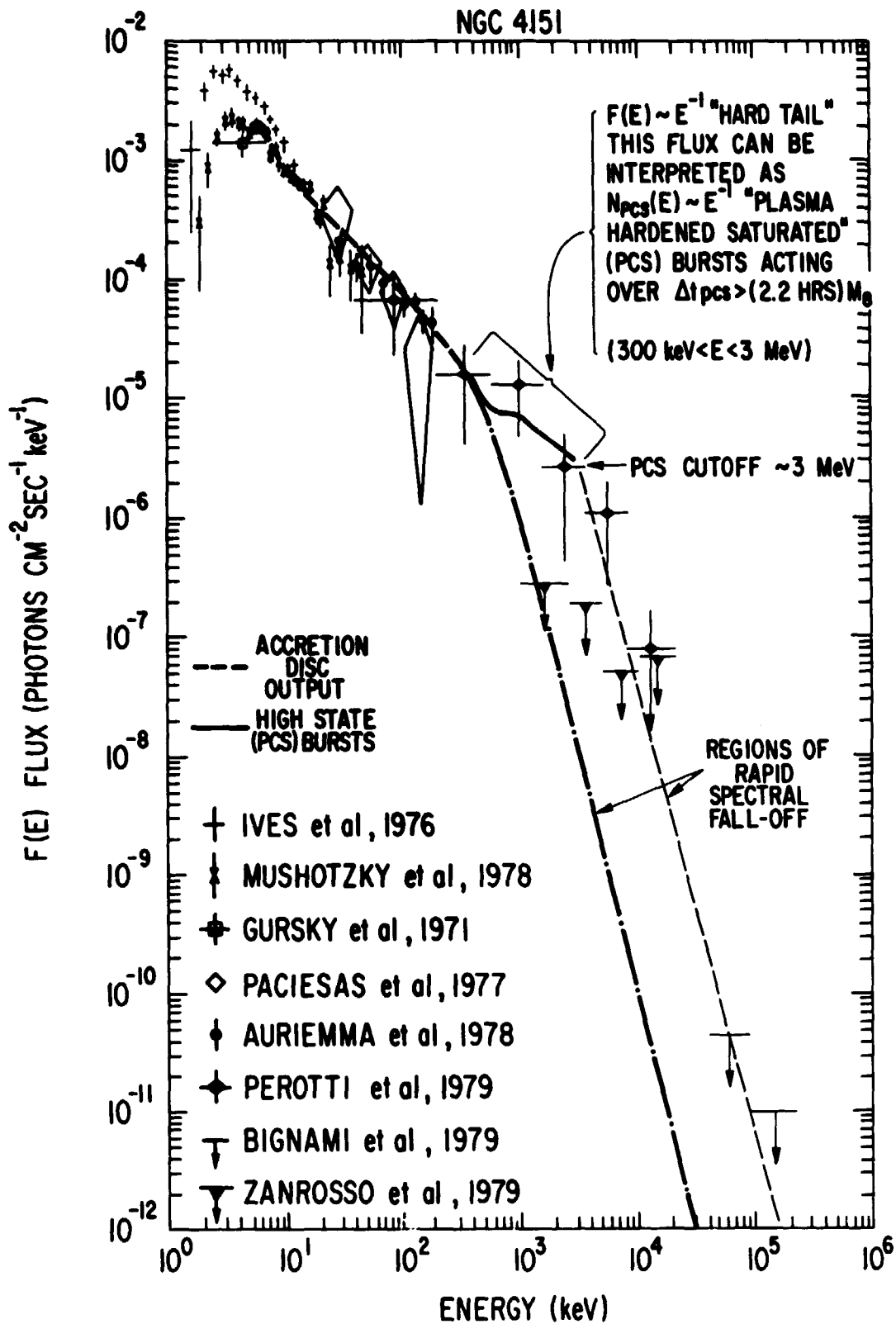


Fig. 6